Appendix 3 Certificate of Analysis (Certification No. B120714-001)

Certification No. B120714-001

Certificate of Analysis

February 8, 2013
Kashima Laboratory
Mitsubishi Chemical Medience Corporation

Chief Analyst: Kunihiro Konno
Kunihiro Konno

Analyst: Junko Ohnuki

Study No.:	B120714
Test Substance:	P092
Lot No.:	7J7XB
GLP:	MHW, Ordinance No. 21, "Standards for Conduct of Nonclinical Studies on the Safety of Drugs" (Dated March 26, 1997; partial revision: Ordinance No. 114, MHLW, dated June 13, 2008)
Description of Analysis:	Confirmation of stability of P092 in preparations [Vehicle: Dimethyl sulfoxide] (Nominal concentration: 0.005 mg/mL and 50 mg/mL)
Analysis:	HPLC
Storage Conditions:	The preparations were stored at room temperature (18.7°C to 20.1°C) and shielded from light in tight container for 24 hours.
Date of Preparation:	November 20, 2012
Date of Analysis:	November 20 and 21, 2012
Results:	The concentrations of P092 in the preparations are shown in the table below. Results indicated that the preparations were stable under the storage conditions.

Concentration \ Date		November 20, 2012	November 21, 2012
		Initial	After 24 hours
0.005 mg/mL	Measured concentration	0.00532 0.00522	0.00538 0.00539
	Mean	0.00527	0.00539
Ratio to initial concentration (%)		-	102.3
50 mg/mL	Measured concentration	47.4 48.2	50.5 49.9
	Mean	47.8	50.2
Ratio to initial concentration (%)		-	105.0

Ratio to initial concentration, acceptable range: 90% to 110%

Appendix 4 Certificate of Analysis (Certification No. B120714-002)

Certification No. B120714-002

Certificate of Analysis

December 10, 2012
Kashima Laboratory
Mitsubishi Chemical Medience Corporation

Chief Analyst: Kunihiro Konno
Kunihiro Konno

Analyst: Natsumi Iguchi

Study No.:	B120714
Test Substance:	P092
Lot No.:	7J7XB
GLP:	MHW, Ordinance No. 21, "Standards for Conduct of Nonclinical Studies on the Safety of Drugs" (Dated March 26, 1997; partial revision: Ordinance No. 114, MHLW, dated June 13, 2008)
Description of Analysis:	Confirmation of concentration of P092 in preparations [Vehicle: Dimethyl sulfoxide] (Nominal concentration: 0.00625 mg/mL and 1.6 mg/mL)
Analysis:	HPLC
Date of Analysis:	December 5, 2012
Results:	The concentrations of P092 in the preparations are shown in the table below. We confirmed that the obtained data were within the acceptable range.[a]

Nominal concentration (mg/mL)	Measured concentration (mg/mL)	Mean (mg/mL)	Ratio to nominal concentration (%)
0.00625	0.00663 0.00672	0.00668	106.9
1.6	1.62 1.66	1.64	102.5

a: Ratio to nominal concentration, acceptable range: 90% to 110%

Appendix 5　背景データ

短時間処理法-S9 mix

データ数	42			
群	陰性対照		陽性対照 (MMC 0.1μg/mL)	
	構造異常（%）	数的異常（%）	構造異常（%）	数的異常（%）
平均	0.3	0.0	37.5	0.1
標準偏差（SD）	0.5	0.2	10.1	0.3
＋2SD	1.3	0.4	57.7	0.7
－2SD	(0)	(0)	17.3	(0)
最大値	1	1	57	1
最小値	0	0	19	0

短時間処理法+S9 mix

データ数	44			
群	陰性対照		陽性対照 (BP 10μg/mL)	
	構造異常（%）	数的異常（%）	構造異常（%）	数的異常（%）
平均	0.1	0.2	26.4	0.1
標準偏差（SD）	0.4	0.5	10.0	0.3
＋2SD	0.9	1.2	46.4	0.7
－2SD	(0)	(0)	6.4	(0)
最大値	2	2	50	1
最小値	0	0	10	0

連続処理法24時間処理

データ数	34			
群	陰性対照		陽性対照 (MMC 0.05μg/mL)	
	構造異常（%）	数的異常（%）	構造異常（%）	数的異常（%）
平均	0.5	0.1	32.9	0.0
標準偏差（SD）	0.8	0.3	12.6	0.2
＋2SD	2.1	0.7	58.1	0.4
－2SD	(0)	(0)	7.7	(0)
最大値	3	1	57	1
最小値	0	0	10	0

(0):負の値となるため，0とする.

信 頼 性 保 証 証 明 書

試験委託者　：　岐阜大学
表　　題　：　P092 のほ乳類培養細胞を用いる染色体異常試験
試 験 番 号　：　B120714

本試験は下記の基準に従って実施され，本最終報告書は，試験の方法，結果が正確に記載されていることを保証する．調査の内容，調査日および報告日を以下に示す．

厚生省令第21号 「医薬品の安全性に関する非臨床試験の実施の基準に関する省令」
（平成9年3月26日，一部改正　厚生労働省令第114号，平成20年6月13日）

調 査 内 容	調査日	報告日	
		試験責任者	運営管理者
試験計画書			
試験計画書	2012年11月13日	2012年11月13日	2012年11月13日
(再調査)	2012年11月14日	2012年11月14日	2012年11月14日
試験計画書変更書 (1)	2012年11月14日	2012年11月14日	2012年11月14日
試験計画書変更書 (2)	2012年11月19日	2012年11月19日	2012年11月19日
試験計画書変更書 (3)	2012年12月03日	2012年12月03日	2012年12月03日
試験計画書変更書 (4)	2013年03月06日	2013年03月06日	2013年03月06日
試験実施状況			
被験物質溶液の安定性分析	2012年11月15日	2012年11月15日	2012年11月15日
被験物質溶液の調製	2012年11月21日	2012年11月21日	2012年11月21日
被験物質溶液の濃度分析	2012年12月05日	2012年12月05日	2012年12月05日
細胞処理	2012年12月06日	2012年12月06日	2012年12月06日
標本作製,細胞増殖率の測定	2012年12月07日	2012年12月07日	2012年12月07日
標本観察	2012年12月14日	2012年12月14日	2012年12月14日
試験資料・最終報告書			
試験資料・最終報告書草案	2013年02月01日 ～2013年02月06日	2013年02月06日	2013年02月06日
(再調査)	2013年02月07日	2013年02月07日	2013年02月07日
(再調査)	2013年02月08日	2013年02月08日	2013年02月08日
試験資料・最終報告書	2013年03月08日	2013年03月08日	2013年03月08日

2013 年 3 月 8 日

信頼性保証部門責任者　東川国男　印

東川 国男
三菱化学メディエンス株式会社
鹿島研究所

［ II ］分担研究報告

厚生労働科学研究費補助金 難治性疾患等克服研究事業（難治性疾患克服研究事業）
プリオン病に対する低分子シャペロン治療薬の開発　分担研究報告書

プリオン病の自然歴調査と低分子シャペロン化合物による治療

研究分担者：水澤英洋　東京医科歯科大学大学院脳神経病態学(神経内科学)
研究代表者：桑田一夫　岐阜大学人獣感染防御研究センタープリオン研究部門
研究協力者：山田正仁　金沢大学医薬保健研究域医学系脳老化･神経病態学(神経内科学)
研究協力者：堂浦克美　東北大学大学院医学系研究科プリオン蛋白分子解析分野
研究協力者：坪井義夫　福岡大学神経内科
研究協力者：岩崎　靖　愛知医科大学加齢医科学研究所
研究協力者：佐藤克也　長崎大学医歯薬学総合研究科感染分子
研究協力者：浜口　毅　金沢大学医薬保健研究域医学系脳老化･神経病態学(神経内科学)
研究協力者：三條伸夫　東京医科歯科大学大学院脳神経病態学(神経内科学)

研究要旨　プリオン病はまだ発症機序が解明されておらず、いくつかの臨床試験は行われたものの有効な治療法もないため、わが国で開発されたプリオン蛋白の物理化学的解析に基づいた新規合成化合物 P092 の効果が期待されている。今年度は、P092 のファースト・イン・ヒューマンの治験を開始するため、プリオン病の患者登録ならびに自然歴調査を含む臨床研究体制として日本プリオン病コンソーシアム(Japanese Consortium of Prion Disease: JACOP)を構築した。そして、治験の開始に向けて、プロトコールの作成と患者登録・追跡調査を開始した。

A.研究目的

本研究の目的は、①P092 のヒトへの投与が可能となった際に全国規模のファースト・イン・ヒューマンの治験を開始できるようにするために、患者登録とフォローアップを含む臨床研究体制を構築する、そのために、その体制を活用して、②我が国におけるプリオン病の各病型の自然歴を明らかにする、ことである。

B. 研究方法

1) プリオン病臨床研究体制の構築

わが国のプリオン病患者は毎年 150 名程度の発生があり、特定疾患としての医療券は約 500 件発行されているのみである。100 万人に 1 名の発症と言われるようにきわめて希な疾患である。したがって、臨床試験を行うには全国規模で患者を組み入れなければ研究に必要な数を確保できない。幸い、厚労省の難治疾患克服研究事業「プリオン病のサーベイランス及び感染予防に関する調査研究班」では、全国を網羅したサーベイランス体制を有しており、全国規模の臨床研究体制の構築にはきわめて有用である。当該研究班および「プリオン病および遅発性ウイルス感染症に関する調査研究班」との緊密な連携により、臨床研究体制を構築する。

2) プリオン病臨床研究体制の活用

わが国では 1999 年 4 月より、プリオン病に関する全国レベルでのサーベイランス調査が続けられており、年 2 回のサーベイランス委員会で新たな症例が認定されている。これまでに 3664 件を調査し、本邦患者の約 90%に達すると思われる 1894 人（男：810 人、女：1,084 人）が認定されており、そのデータから、わが国では人口 100 万人対の罹患率は 1.01 人で欧米の罹患率と同等で、発病時の平均年齢は 67.8 歳であることが判明している。わが国における現行の医療制度においては治療法のないプリオン病などの難治性疾患を特定の医療機関で長期にフォローすることは不可能に等しく、サーベイランス調査ではプリオン病の自然歴が把握できていないため、わが国におけるプリオン病の

罹患率は明らかとなったが、自然歴に関しては依然として解明されていない。プリオン病の代表的疾患である古典型孤発性クロイツフェルト・ヤコブ病は発症から 3〜6 ヶ月で無動性無言になることが知られているが、このような大まかなデータでは、将来治療薬試験を開始したとしても効果判定をすることができない。

そこで、構築されたプリオン病臨床研究体制を活用して、プロトコールを作成した上で患者登録とそのフォローアップを行い、自然癒を解明する。

（倫理面への配慮）

疫学的・臨床研究に際しては、それぞれの疾患の患者や家族からインフォームドコンセントを得て個人情報の守秘を計るとともに、実験動物を使用する研究においてもそれぞれの施設の定める手続きに従って動物愛護に十分留意して実施する。サーベイランスについては委員長の所属施設にて倫理審査を受け承認されている。

C. 研究結果

1) プリオン病臨床研究体制の構築

プリオン蛋白の物理化学的構造解析から開発された化合物GN8を修飾・発展させたP092がプリオン蛋白へ結合し、その構造変換を抑制することより、プリオン蛋白の異常化が抑制でき、治療薬として期待が高まっている。P092のヒトへの投与が可能となったときに、迅速にファースト・イン・ヒューマンの治験を行うために、臨床研究体制を構築する必要がある。

プリオン病のサーベイランスおよび感染予防に関する研究班とプリオン病および遅発性ウイルス感染症に関する調査研究班の臨床系班員を中心に参加を求め、わが国におけるプリオン病の研究に関するコンソーシアム、日本プリオン病研究紺ソーシアム（Japanese Consortium of Prion Disease: JACOP）を設立した（**図1**）。JACOPの運営は、運営委員会を設けて、そこでの話し合いによって行う。

2) プリオン病臨床研究体制の活用

プリオン病は、前述のようにきわめて希であり、かつ多くは発症後1年程度で死に至るきわめて進行の早い疾患である。したがって、患者登録には全国に呼びかけて参加を求めることが必要であり、そのプロトコールはプリオン病の臨床的特徴を網羅し、急速な進行に対応したものとすることとなった。このようにして、まずプリオン病各病型の自然歴を明らかにし、必要に応じて臨床試験の際のコントロールとして使えるようにする。具体的には東京医科歯科大学にJACOPの事務局とデータセンターを設置し、運営委員の所属する東北大学、福井大学、金沢大学、愛知医科大学、長崎大学が中心となってJCOPを周知してゆくこととなった。同時に、登録患者のリンパ球、脳脊髄髄液、血清などを保存できるようにサンプル保管室、培養細胞保管室内に、本研究目的の超低温槽、細胞保管容器を設置し、超低温槽に関しては、2011年3月の大震災の教訓より、2施設（本学、および東京都健康長寿医療センター）に同一検体を分散して保管できるように超低温槽を整備し、患者サンプルの保管を開始した。

D. 考察

国内外において、プリオン病の罹患率は人口100万人あたり年間1人であることが明らかになっているが、国内外を問わず、これまでにプリオン病における正確な自然歴を調査された報告はない。今回の課題の治験薬の臨床試験のためにはもちろん、プリオン病の発症機序の理解のためにも、正確な自然歴調査は必要不可欠で有り、JACOP構築の意義はきわめて大きい。

JACOPの構築により、治験に応用可能な自然歴調査のプロトコールの作成ができ、さらに調査体制、試料保存体制も整備でき、自然歴調査による患者登録を開始することができた。今後、治験開始準備と平行して、登録患者を増やし、定期的な追跡調査を行ってゆく予定である。以上より、P092のヒトへの投与が可能となったときに、迅速かつスムーズにファースト・イン・ヒューマンの治験を開始することができると期待される。

E. 結論

わが国におけるオールジャパンのプリオン病の研究体制であるJACOPを構築し、プロト

コールを作成、自然歴調査を確立した。今後は世界初のプリオン蛋白の物理化学的解析に基づき作製された新規化合物 P092 を用いた治験の準備を進めながら、自然歴調査を継続、JACOP を強化してゆく。

[参考文献]

なし

F. 健康危険情報

なし。

G. 研究発表（2012/4/1～2013/3/31 発表）

1. 論文発表

[雑誌]

1) Fujita K, Harada M, Sasaki M, Yuasa T, Sakai K, Hamaguchi T, Sanjo N, Shiga Y, Satoh K, Atarashi R, Shirabe S, Nagata K, Maeda T, Murayama S, Izumi Y, Kaji R, Yamada M, Mizusawa H. Multicentre, multiobserver study of diffusion-weighted and fluid-attenuated inversion recovery MRI for the diagnosis of sporadic Creutzfeldt-Jakob disease: a reliability and agreement study. BMJ Open 2(1): e000649, 2012
2) Yoshikawa Y, Horiuchi M, Ishigura N, Kadohira M, Kai S, Mizusawa H, Nagata C, Onodera T, Sata T, Tsutsui T, Yamada M, Yamamoto S. Alternative BSE risk assessment methodology for beef and beef offal imported into Japan. J Vet Med Sci 74(8): 959-968, 2012
3) Takumi Hori, Nobuo Sanjo, Makoto Tomita, Hidehiro Mizusawa. Visual Reproduction on the Wechsler Memory Scale-Revised as a predictor of Alzheimer's disease in Japanese patients with mild cognitive impairments. Dementia and Geriatric Cognitive Disorders 35(3-4): 165-76, 2013
4) Maya Higuma, Nobuo Sanjo, Katsuya Satoh, Yusei Shiga, Kenji Sakai, Ichiro Nozaki, Tsuyoshi Hamaguchi, Yosikazu Nakamura, Tetsuyuki Kitamoto, Susumu Shirabe, Shigeo Murayama, Masahito Yamada, Jun Tateishi, Hidehiro Mizusawa. Relationships between Clinicopathological Features and Cerebrospinal Fluid Biomarkers in Japanese Patients with Genetic Prion Diseases. PLoS One 8(3): e60003, 2013
5) Sano K, Satoh K, Atarashi R, Takashima H, Iwasaki Y, Yoshida M, Sanjo N, Murai H, Mizusawa H, Schmitz M, Zerr I, Kim YS, Nishida N. Early Detection of Abnormal Prion Protein in Genetic Human Prion Diseases Now Possible Using Real-Time QUIC Assay. PLoS One 8(1): e54915, 2013

2. 学会発表

1) Sanjo N, Nakamura Y, Kitamoto T, Yamada M, Hamaguchi T, Moriwaka F, Aoki M, Kuroiwa Y, Nishizawa M, Takeda M, Inuzuka T, Abe K, Mrai H, Murayama S, Satoh K, Harada M, Saito N, Takumi I, Mizusawa H. Human prion diseases in Japan: aprospective surveillance from 1999. Asian Pacific Prion Symposium 2012, Yokohama, July 29-30, 2012.
2) Sakai K, Hamaguchi T, Noguchi-Shinohara M, Nozaki I, Sato T, Takumi I, Sannjo N, Nakamura Y, Kitamoto T, Saito N, Mizusawa H, Yamada M. Prion protein propagation in dura mater graft-associated Creutzfeldt-Jakob disease. Asian Pacific Prion Symposium 2012, Yokohama, July 29-30, 2012.
3) Sakai K, Hamaguchi T, Noguchi-Shinohara M, Nozaki I, Sato T, Takumi I, Sanjo N, Nakamura Y, Kitamoto T, Saito N, Mizusawa H, Yamada M. Prion protein propagation in dura mater graft-associated Creutzfeldt-jakob disease. Prion2012, Amsterdam, May 10-12, 2012.
4) Sanjo N, Ohara M, Satoh K, Hamaguchi T, Nakamura Y, Kitamoto T, Yamada M, Mizusawa H. Clinical features of genetic prion disease and cerebrospinal fluid findings in Japanese patients. Prion2012, Amsterdam, May 10-12, 2012.
5) Mizusawa H. PrionDiseases in Japan.The 13th Ilsong International Symposium CJD Surveillance in Asia.,Ilsong,Feb.13,2012
6) Mizusawa H. PrionDiseases in Japan. National for Viral Disease Control and Prevention. Beijin.Nov.5.2011

なし

H. 知的財産権の出願・登録状況（予定を含む。）

1. 特許取得

なし

2. 実用新案登録

なし

3. その他

なし

図 1

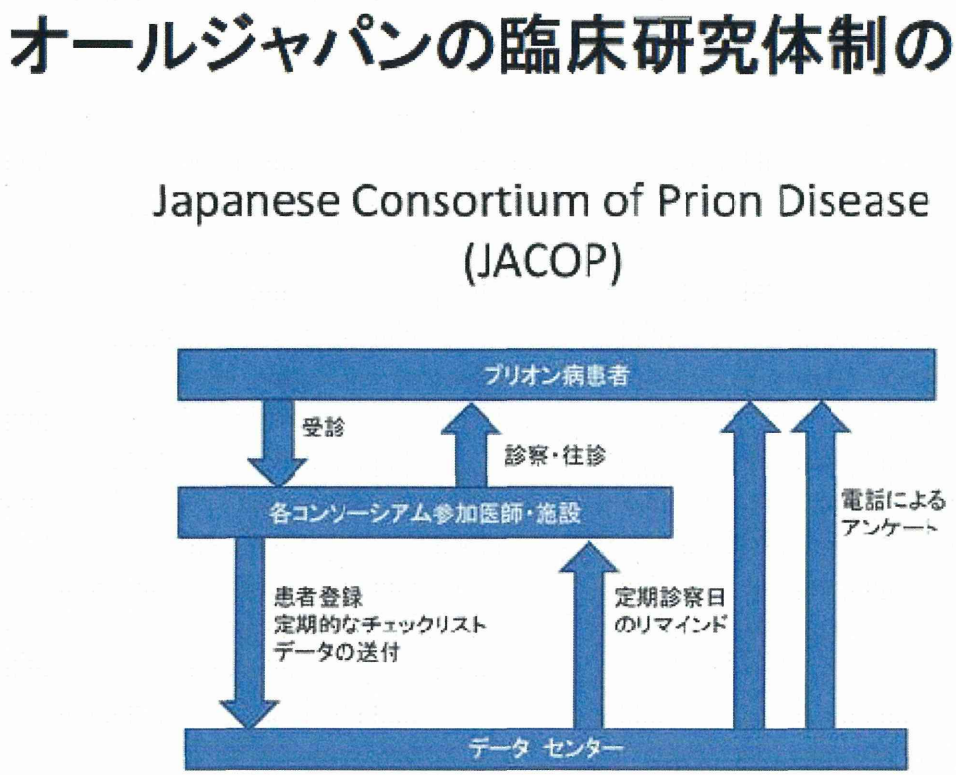

［ III ］研究成果の刊行に関する一覧表

研究成果の刊行に関する一覧表

雑誌（英文原著）

1	発表者氏名	Le Chang, Takeshi Ishikawa, Kazuo Kuwata, Shoji Takada.						
	論文タイトル名	Protein-specific force field derived from the fragment molecular orbital method can improve protein-ligand binding interactions.						
	発表誌名	Journal of Computational Chemistry	巻号	34(14)	ページ	1251-1257	出版年	2013
2	発表者氏名	T. Ishikawa, R. R. Burri, Yuji O. Kamatari, S. Sakuraba, N. Matubayasi, A. Kitao, K. Kuwata.						
	論文タイトル名	A theoretical study of the two binding modes between lysozyme and tri-NAG with an explicit solvent model based on the fragment molecular orbital method.						
	発表誌名	Physical chemistry chemical physics	巻号	15(10)	ページ	3646-3654	出版年	2013
3	発表者氏名	K. Takemura, R. R. Burri, T. Ishikawa, T. Ishikura, S. Sakuraba, N. Matubayasi, K. Kuwata, A. Kitao.						
	論文タイトル名	Free-energy analysis of lysozyme-triNAG binding modes with all-atom molecular dynamics simulation combined with the solution theory in the energy representation.						
	発表誌名	Chemical physics letters	巻号	559	ページ	94-98	出版年	2013
4	発表者氏名	Mashima Tsukasa, Nishikawa Fumiko, Kamatari Yuji, Fujiwara Hiromichi, Saimura Masayuki, Nagata Takashi, Kodaki Tsutomu, Nishiwaka Satoshi, Kuwata Kazuo, Katahira Masato.						
	論文タイトル名	Anti-prion activity of an RNA aptamer and its structural basis.						
	発表誌名	Nucleic Acids Research	巻号	41(2)	ページ	1355-1362	出版年	2013
5	発表者氏名	Takuya Okamoto, Takeshi Ishikawa, Yoshiyuki Koyano, Norifumi Yamamoto, Kazuo Kuwata, Masataka Nagaoka.						
	論文タイトル名	A minimal implementation of the AMBER-PAICS interface for Ab initio FMO-QM/MM-MD simulation.						
	発表誌名	Bulletin of the Chemical Society of Japan	巻号	86(2)	ページ	210-222	出版年	2013
6	発表者氏名	Yuji Kamatari, Yosuke Hayano,, Kei-ichi Yamaguchi, Junji Hosokawa-Muto, *Kazuo Kuwata.						
	論文タイトル名	Characterizing antiprion compounds based on their binding properties to prion proteins: Implications as medical chaperones.						
	発表誌名	Protein Science	巻号	22(1)	ページ	22-34	出版年	2013
7	発表者氏名	Ishikawa Takeshi, Kuwata Kazuo.						
	論文タイトル名	RI-MP2 Gradient Calculation of Large Molecules Using the Fragment Molecular Orbital Method.						
	発表誌名	Journal of Physical Chemistry Letters	巻号	3(3)	ページ	375-379	出版年	2012
8	発表者氏名	Kazunori Yamada, Hiroko Koyama, Kyoji Hagiwara, Atsushi Ueda, Yutaka Sasaki, Shin-nosuke Kanesashi, Ryuki Ueno, Hironori K. Nakamura, Kazuo Kuwata, Kazufumi Shimizu, Masaaki Suzuki, Yoko Aida.						
	論文タイトル名	Identification of a novel compound with antiviral activity against influenza A virus depending on PA subunit of viral RNA polymerase.						
	発表誌名	Microbes and Infection	巻号	14(9)	ページ	740-747	出版年	2012
9	発表者氏名	Koji Fujita, Masafumi Harada, Makoto Sasaki, Tatsuhiko Yuasa, Kenji Sakai, Tsuyoshi Hamaguchi, Nobuo Sanjo, Yusei Shiga, Katsuya Satoh, Ryuichiro Atarashi, Susumu Shirabe, Ken Nagata, Tetsuya Maeda, Shigeo Murayama, Yuishin Izumi, Ryuji Kaji, Masahito Yamada, Hidehiro Mizusawa.						
	論文タイトル名	Multicentre, multiobserver study of diffusion-weighted and fluid-attenuated inversion recovery MRI for the diagnosis of sporadic Creutzfeldt-Jakob disease: a reliability and agreement study.						
	発表誌名	BMJ open	巻号	2(1)	ページ	e000649	出版年	2012

10	発表者氏名	Yasuhiro Yoshikawa, Motohiro Horiuchi, Naotaka Ishiguro, Mutsuyo Kadohira, Satoshi Kai, Hidehiro Mizusawa, Chisato Nagata, Takashi Onodera, Tetsutaro Sata, Toshiyuki Tsutsui, Masahito Yamada, Shigeki Yamamoto.						
	論文タイトル名	Alternative BSE risk assessment methodology for beef and beef offal imported into Japan.						
	発表誌名	The Journal of veterinary medical science	巻号	74(8)	ページ	959-968	出版年	2012
11	発表者氏名	Takumi Hori, Nobuo Sanjo, Makoto Tomita, Hidehiro Mizusawa.						
	論文タイトル名	Visual Reproduction on the Wechsler Memory Scale-Revised as a predictor of Alzheimer's disease in Japanese patients with mild cognitive impairments.						
	発表誌名	Dementia and Geriatric Cognitive Disorders	巻号	35(3-4)	ページ	165-176	出版年	2013
12	発表者氏名	Maya Higuma, Nobuo Sanjo, Katsuya Satoh, Yusei Shiga, Kenji Sakai, Ichiro Nozaki, Tsuyoshi Hamaguchi, Yosikazu Nakamura, Tetsuyuki Kitamoto, Susumu Shirabe, Shigeo Murayama, Masahito Yamada, Jun Tateishi, Hidehiro Mizusawa.						
	論文タイトル名	Relationships between Clinicopathological Features and Cerebrospinal Fluid Biomarkers in Japanese Patients with Genetic Prion Diseases.						
	発表誌名	PLoS One	巻号	8(3)	ページ	e60003	出版年	2013
13	発表者氏名	Kazunori Sano, Katsuya Satoh, Ryuichiro Atarashi, Hiroshi Takashima, Yasushi Iwasaki, Mari Yoshida, Nobuo Sanjo, Hiroyuki Murai, Hidehiro Mizusawa, Matthias Schmitz, Inga Zerr, Yong-Sun Kim, Noriyuki Nishida.						
	論文タイトル名	Early Detection of Abnormal Prion Protein in Genetic Human Prion Diseases Now Possible Using Real-Time QUIC Assay.						
	発表誌名	PLoS One	巻号	8(1)	ページ	e54915	出版年	2013

雑誌（和文総説）

1	発表者氏名	桑田一夫						
	論文タイトル名	量子創薬—論理的形態制御学の原理—(Non-commutative Geometrical Drug Discovery —The Principle of Geometrical Regulation—)						
	発表誌名	YAKUGAKU ZASSHI	巻号	132(8)	ページ	873-879	出版年	2012

書籍

なし

［ IV ］研究成果の刊行物・別刷

Protein-Specific Force Field Derived from the Fragment Molecular Orbital Method can Improve Protein–Ligand Binding Interactions

Le Chang,[a,b] Takeshi Ishikawa,[c,d] Kazuo Kuwata,[b,c] and Shoji Takada*[a,b]

Accurate computational estimate of the protein–ligand binding affinity is of central importance in rational drug design. To improve accuracy of the molecular mechanics (MM) force field (FF) for protein–ligand simulations, we use a protein-specific FF derived by the fragment molecular orbital (FMO) method and by the restrained electrostatic potential (RESP) method. Applying this FMO-RESP method to two proteins, dodecin, and lysozyme, we found that protein-specific partial charges tend to differ more significantly from the standard AMBER charges for isolated charged atoms. We did not see the dependence of partial charges on the secondary structure. Computing the binding affinities of dodecin with five ligands by MM PBSA protocol with the FMO-RESP charge set as well as with the standard AMBER charges, we found that the former gives better correlation with experimental affinities than the latter. While, for lysozyme with five ligands, both charge sets gave similar and relatively accurate estimates of binding affinities. © 2013 Wiley Periodicals, Inc.

DOI: 10.1002/jcc.23250

Introduction

Computational study of protein–ligand docking has intensively been performed due to its fundamental roles in rational drug design.[1] In contemporary high-throughput screening, prediction of protein–ligand complex structures and rough estimate of binding affinities often accelerate identification of lead compounds. Yet, the *in silico* screening, at best, increases the probability of finding the lead compounds, but the estimates of individual protein–ligand binding affinities are often poor and less accurate.[2] For better prediction of the protein–ligand docking and binding affinities, simultaneous achievement of high accuracy in energy calculations and efficient sampling in simulations is of central importance. While molecular mechanics (MM) force fields (FFs)[3–5] have been most often used, in practice, the accuracy of the standard FF is limited. Thus, many extensions, such as polarizable FFs,[6] have been developed, but they are somewhat complicated and thus are not very widely applied.

Generally, in developing FF, one tends to consider that FF should be transferable. Once we obtain a set of parameters for an amino acid, for example, the same set of parameters is used for the same type of amino acid in any proteins. Although the transferability may be important for convenience of applications and physical clarity, it is also true that this requirement reduces specificity in the FF. Namely, even for the same type of amino acids, their local environment differ one by one so that the best FF could be different depending on its local environment. If we allow every amino acids to have different parameter values, in principle, this protein-specific FF can give higher accuracy than the standard FF.[7–11] In this article, we address the possibility of protein-specific FF for calculations of protein–ligand binding affinities.

In fact, the idea of protein-specific FF is not brand new. Some years ago, Ji et al.[11] proposed to use protein-specific partial charges. Based on quantum chemical calculations of fragments of a protein, they applied the restrained electrostatic potential (RESP) method to obtain partial charges specific to the protein. By this way, they could incorporate the protein-specific polarization effect. For example, it was shown that several aspartates in lysozyme have quite different partial charges. In their study, they used capped dipeptide fragments for the quantum chemical calculation, which thus did not include protein-wide electronic state changes. Okiyama et al.[12,13] developed the RESP protocol for the fragment molecular orbital (FMO)-based electrostatic potential for proteins/polypeptides to determine partial charges. The FMO method can approximately calculate the electronic energy of an entire protein in terms of molecular orbitals of fragments and fragment pairs, which drastically speeds up the calculation of the electronic states of entire proteins. By using the FMO method, they could compute the electronic state of entire proteins, which was fed into the RESP procedure. They showed promising result in the accuracy of molecular dynamics (MD) simulations.

[a] L. Chang, S. Takada
Department of Biophysics, Graduate School of Science, Kyoto University, Kyoto 6068502, Japan
E-mail: takada@biophys.kyoto-u.ac.jp
[b] L. Chang, K. Kuwata, S. Takada
CREST Japan Science and Technology Agency
[c] T. Ishikawa, K. Kuwata
Center for Emerging Infectious Diseases, Gifu University, Gifu 5011193, Japan
[d] T. Ishikawa
Graduate School of Engineering, Tohoku University, Sendai 9808579, Japan

In this study, we put forward the Okiyama et al.'s method towards the protein–ligand docking problem using the protein-specific FF based on FMO calculation together with the RESP method. This article is organized in the followings. The Methodology section briefly describes our protocols, which rely on the FMO calculation of proteins and use the RESP method with restraint to the AMBER charges to set up the protein-specific partial charges. In Results, we first apply the method for two proteins, dodecin, and lysozyme to determine the partial charges. Next, how partial charges depend on the local environment is analyzed. Finally, we test the protein-specific FF for the estimate of binding affinity using the simple MM PBSA method. The article ends with brief Discussions and Conclusions.

Methodology

To obtain the atomic partial charges for a particular conformation of a particular protein, we need the electrostatic potential around the protein surface computed by *ab initio* quantum mechanics (QM). Here, we used the FMO method[14,15] for this purpose. In this method, a large biopolymer (protein, DNA, RNA, etc.) is divided into many fragments. At the dimeric level of accuracy, the interaction energies of fragment pairs (dimer), whose distance is close enough (less than twice the sum of van der Waals radii for the closest pair of atoms) in a certain conformation, are also calculated. The total energy of the biopolymer corresponding to a specific conformation is

$$E = \sum_{I=1}^{N} E_I + \sum_{I<J} (E_{IJ} - E_I - E_J), \tag{1}$$

where $I(IJ)$ is the suffix for monomer (dimer), N is the total number of monomers in the system, E_I and E_{IJ} are the Ith fragment energies, and the IJ fragment pair energies.[14,15] The electrostatic potential around the protein surface could be obtained by the similar formula. The electrostatic potential $V(\vec{r})$ at a specific point $\vec{r}$ is

$$V(\vec{r}) = \sum_{I=1}^{N} V(\vec{r})_I + \sum_{I<J} [V(\vec{r})_{IJ} - V(\vec{r})_I - V(\vec{r})_J]. \tag{2}$$

The calculation of the electrostatic potential is implemented in GAMESS.[16,17] In particular, we used Hartree–Fock method with the 6-31G* basis set in computing the molecular orbitals. Currently, GAMESS could not directly output the FMO electrostatic potential at specific point in space. However, it is able to output the electrostatic potential of all monomers and dimers at specific point in space. Therefore, the FMO electrostatic potential at specific point in space could be obtained by eq. (2) and GAMESS output data in FMO calculation. In this work, the source code of GAMESS is modified to output enough number of electrostatic potential points. A program is coded to compute the FMO electrostatic potential from GAMESS output data in FMO calculation.

After the electrostatic potential around a protein surface is obtained, the partial charge of each atom in the protein could be fitted using the RESP method.[18] In the RESP fitting, new partial charges q_i could be obtained by minimizing the penalty function χ^2 given as

$$\chi^2 = \sum_{j=1}^{N_{\text{point}}} (V_j - V_{0j})^2 + k \sum_{i=1}^{N_{\text{atom}}} (q_i - q_{0i})^2, \tag{3}$$

where V_j and V_{0j} represent the electrostatic potential calculated by MM and QM, q_i and q_{0i} stand for the fitted partial charges and the restrained partial charges, N_{point} and N_{atom} are the numbers of electrostatic potential points and atoms for fitting, and k is the weight factor that modulates the strength of restraint. For proteins, partial charges are restrained to AMBER 94 charges with the weight factors calculated by Okiyama's equation[12,13]

$$k = \sum_{j=1}^{N_{\text{point}}} (V_{0j} - \bar{V}_0)^2 / \sum_{i=1}^{N_{\text{atom}}} (q_{0i} - \bar{q}_0)^2, \tag{4}$$

where $\bar{V}_0 = (\sum_{j=1}^{N_{\text{point}}} V_{0j})/N_{\text{point}}$ and $\bar{q}_0 = (\sum_{i=1}^{N_{\text{atom}}} q_{0i})/N_{\text{atom}}$. For ligands, the fitting is performed in two steps. First, the partial charges are restrained to zero partial charges with the weight factors set to $k = 0.001$. In the second stage, the partial charges are restrained to those obtained from the first stage fitting with the weight factor calculated by Okiyama's equation. The RESP fitting is performed by the R.E.D program.[19]

In this work, using the native structure of target proteins without a ligand, after energy minimization procedure with the AMBER 94 FF,[3,4] we obtain the partial charges of atoms in two proteins, dodecin, and lysozyme. In consistent with the procedure used in AMBER charge determination, we put the molecule in vacuum and did not include any solvation effect. Using thus obtained FF as well as the standard AMBER FF, we performed MD simulations for dodecin, its five ligands, and the five protein–ligand complexes for 10 nanoseconds using AMBER package.[20] In the same way, we conducted MD simulations for lysozyme, its five ligands, and the five protein–ligand complexes. Then, the binding free energies are calculated by the MM PBSA approach[21] according to the three MD trajectories.

Results

We first calculated protein-specific partial charges by the FMO-RESP method at the native structures of two proteins, dodecin (pdb code 2CC9), and hen egg-white lysozyme (pdb code 1LZA). Then, the free energies of five ligands binding to dodecin and lysozyme are calculated by the FMO-RESP charges and by using the standard AMBER charges.

Partial charges and local environment

Since the FMO-based partial charges are fitted with the restraint to the AMBER charges, the value of $Q_{\text{FMO}} - Q_{\text{AMBER}}$ is used to scale the variation of partial charge. Here, Q_{FMO} stands for the partial charges derived from the FMO-RESP fitting to

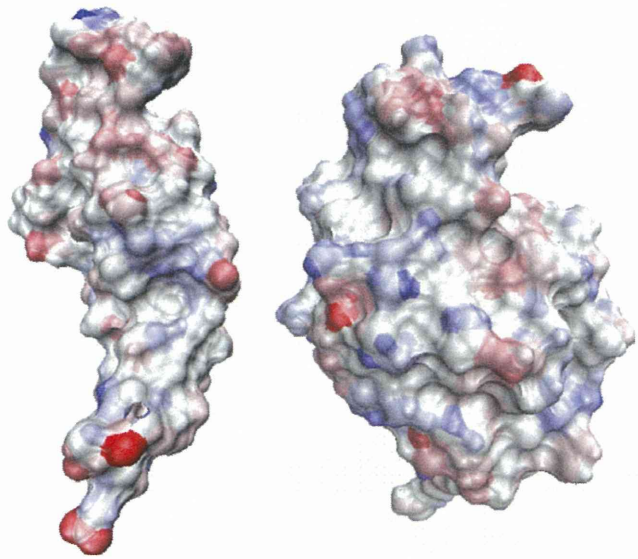

Figure 1. The partial charge variation of surface atoms. The structure in the left corresponds to dodecin, whereas the one in the right corresponds to lysozyme. Color indicates the value of charge variation: red means $Q_{FMO} < Q_{AMBER}$, whereas blue means $Q_{FMO} > Q_{AMBER}$.

electrostatic potentials of FMO calculation, Q_{AMBER} stands for the AMBER 94 partial charges.

Figure 1 shows the partial charge variations ($Q_{FMO} - Q_{AMBER}$) of surface atoms. The structure in the left corresponds to dodecin, whereas the one in the right corresponds to lysozyme. Color indicates the value of charge variation: red means $Q_{FMO} < Q_{AMBER}$, whereas blue means $Q_{FMO} > Q_{AMBER}$. In the case of dodecin, which has negative net charges of −12e, the charge variations of surface atoms tend to be negative (red colored). Conversely, for the positively charged lysozyme with net charges of +8e, there are more blue colored points on the surface.

The reason that causes partial charge alteration of an atom is its neighbor atoms. Once an atom is close to its neighbor atoms in space, charges on it could be transferred to its neighbors. Therefore, the partial charge of an atom will be influenced by the properties of and distances to its neighbor atoms. For an atom, the properties of and distances to its neighbor atoms could be termed as 'local environment' in the following discussions. To measure the contribution of local environment to charge transfer, the 'charge transfer factor' F_{CT} is defined to estimate the amount of charge transfer from all other atoms (j) to specific atom (i).

$$F_{CT}(i) = \sum_{j=1(j\neq i)}^{N_{atom}} e^{-\frac{1}{2}\left(\frac{d_{ij}}{d_0}\right)^2}, \quad (5)$$

where d_{ij} is the distance between atom i and j and d_0 gives the cutoff distance for charge transfer. Since charge is constrained in the van der Waals radii of atom in MM simulation, the average value of van der Waals radii is used to approximate d_0, which gives

$$d_0 = 2\frac{\sum_{i=1}^{N_{atom}} r_i}{N_{atom}}, \quad (6)$$

where r_i is the van der Waals radii of atom i. For an atom, if the value of F_{CT} is large, it has more neighbor atoms nearby.

Figure 2a plots the partial charge variation ($Q_{FMO} - Q_{AMBER}$) as a function of local environment (F_{CT}). Interestingly, the atoms which have larger charge variation (either positive or negative) tend to appear in the region corresponding to smaller charge transfer factors. The partial charge variations of atoms which have larger charge transfer factors converge to zero. In other words, the partial charge for an atom buried inside which has more neighbor atoms nearby is close to AMBER charge. Conversely, the partial charge for an atom near the surface which do not have much neighbor atoms nearby tend to has larger deviation from AMBER charge. Since such deviation could be either positive or negative, the correlation coefficient between $Q_{FMO} - Q_{AMBER}$ and F_{CT} is small (0.04). If $Q_{FMO} - Q_{AMBER}$ is replaced by its absolute value, the correlation coefficient between $|Q_{FMO} - Q_{AMBER}|$ and F_{CT} has significant larger value of 0.49 (as shown in Fig. 2b).

The absolute values of partial charge variation as a function of local environment are also investigated for different types of atoms (oxygen in Fig. 3a, nitrogen in Fig. 3b, carbon in Fig.

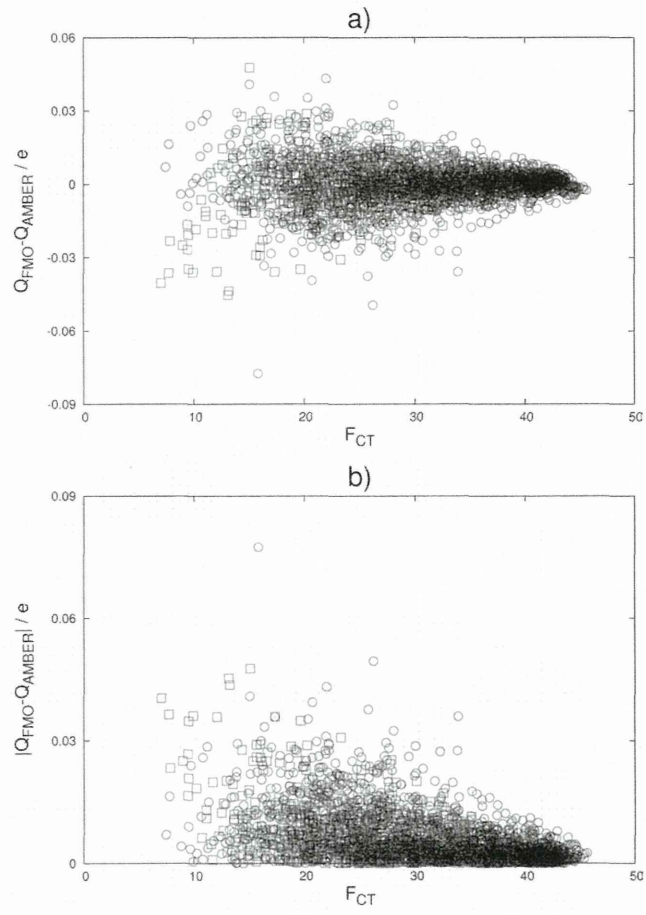

Figure 2. a) The value of partial charge variation as a function of charge transfer factor with data from both dodecin (square) and lysozyme (circle). The corresponding correlation coefficient is: 0.04 (0.19 for squares, −0.03 for circles). b) The absolute value of partial charge variation as a function of charge transfer factor with data from both dodecin (square) and lysozyme (circle). The corresponding correlation coefficient is: −0.49 (−0.50 for squares, −0.49 for circles).

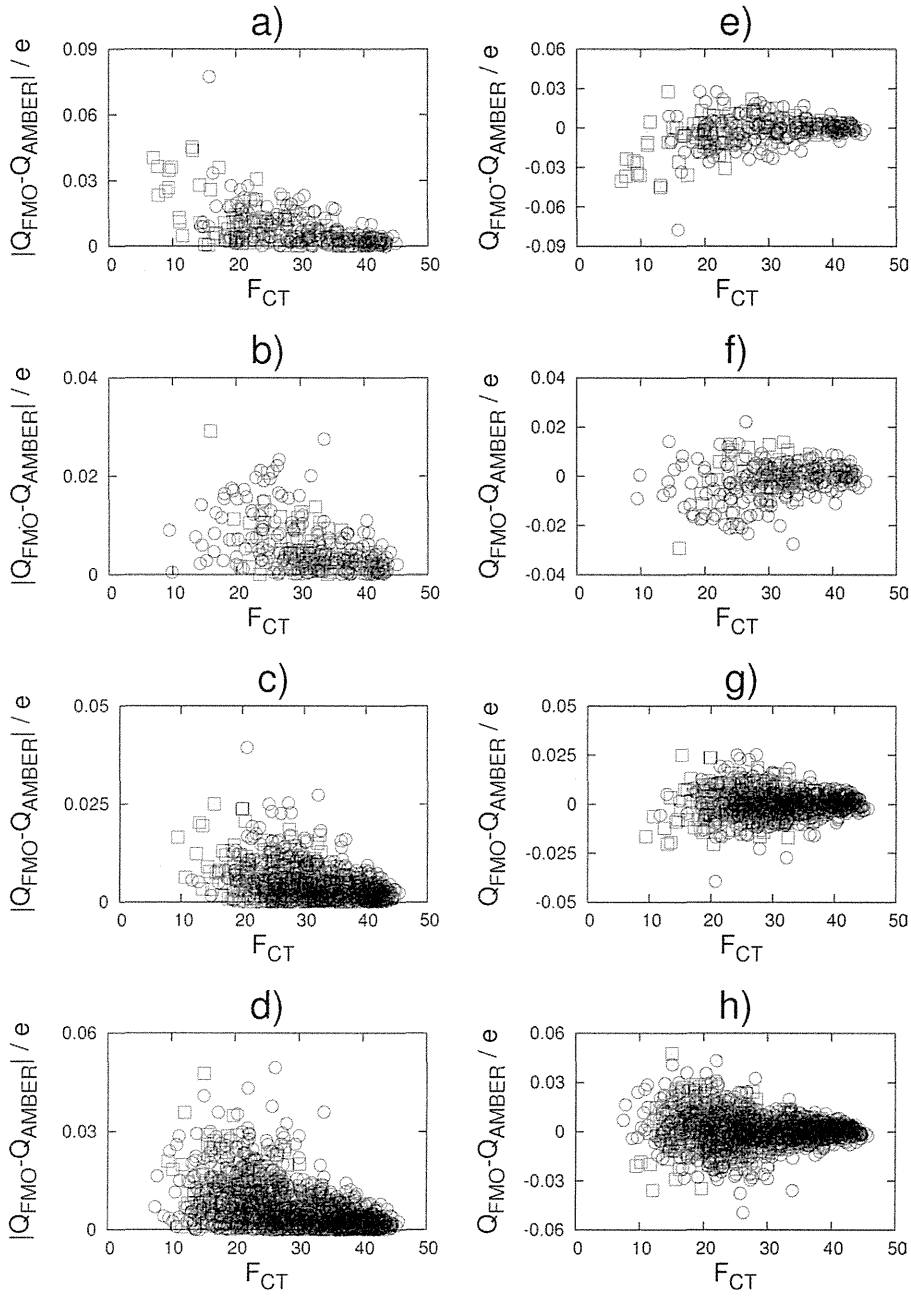

Figure 3. The absolute value of partial charge variation as a function of charge transfer factor, for oxygen a), nitrogen b), carbon c), and hydrogen d) atoms with data from both dodecin (square) and lysozyme (circle). The corresponding correlation coefficients are: −0.56 (−0.60 for squares, −0.51 for circles), −0.44 (−0.42 for squares, −0.45 for circles), −0.39 (−0.41 for squares, −0.38 for circles), and −0.50 (−0.48 for squares, −0.51 for circles). And the partial charge variation as a function of charge transfer factor, for oxygen e), nitrogen f), carbon g), and hydrogen h) atoms with data from both dodecin (square) and lysozyme (circle). The corresponding correlation coefficients are: 0.37 (0.53 for squares, 0.21 for circles), 0.26 (0.35 for squares, 0.25 for circles), 0.04 (0.12 for squares, 0.00 for circles), and −0.09 (0.05 for squares, −0.16 for circles).

3c, and hydrogen in Fig. 3d) separately. It is found that oxygen atoms with small F_{CT} have largest absolute values of charge variations, hydrogen atoms with small F_{CT} have the second largest absolute values of charge variations, whereas carbon and nitrogen atoms with small F_{CT} have relative smaller absolute values of partial charge variations. Such phenomenon could be explained by the ability to obtain charge of certain type of atom. Oxygen atom has strong tendency to attract electron and obtain negative charge, whereas hydrogen atom has strong tendency to lose electron and obtain positive charge. Since oxygen and hydrogen atoms could obtain more charges, they tend to possess more charges when isolated from neighbor atoms and have more deviations from AMBER charges. Such explanation is supported by the plots of partial charge variation as a function of local environment for different types of atoms (oxygen in Fig. 3e, nitrogen in Fig. 3f, carbon in Fig. 3g, and hydrogen in Fig. 3h). For oxygen and nitrogen atoms, the correlation coefficients between $Q_{FMO} - Q_{AMBER}$ and F_{CT} have positive values, revealing the fact that they tend to be negatively charged. While for hydrogen atoms, the

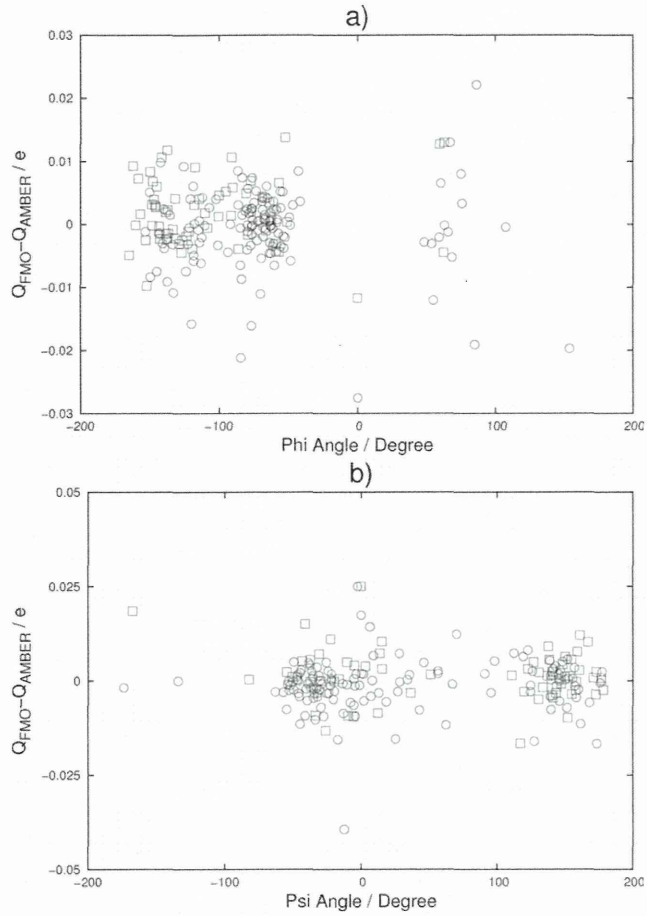

Figure 4. The partial charge variation as a function of backbone dihedral angles phi a) and psi b) with data from both dodecin (square) and lysozyme (circle).

correlation coefficient between $Q_{FMO} - Q_{AMBER}$ and F_{CT} have negative values, indicating that they tend to be positively charged. However, there is no atom completely isolated from neighbor atoms in protein structure. Therefore, the value of partial charge variation ($Q_{FMO} - Q_{AMBER}$) for an atom with small F_{CT} value is sensitive to the charge properties of its neighbor atoms. That might be the reason why atoms with small F_{CT} have a wide range of $Q_{FMO} - Q_{AMBER}$ values. According to the above results, isolated negatively charged atoms tend to keep more electrons, isolated positively charged atoms tend to keep more positive charges and isolated neutral atoms tend to keep neutral. Such feature about charged atoms agrees with the result of a previous FMO calculation for protein–water interaction energy by Ishikawa and Kuwata.[22] In that article, the protein–water interaction of charged residues related to salt bridges is weaker than that of charged residues not related to salt bridges.

The dependence of charge distribution on local secondary structure can be very important for molecular modeling of protein. Figure 4 gives the deviation of FMO charges from AMBER charges of backbone atoms in relation to backbone dihedral angles (a, Phi vs. nitrogen and b, Psi vs. carbon), which are indices for local secondary structures. According to the figures, there seems no apparent correlation between the charge variation and the secondary structures. This is not surprising since most of backbone atoms are neutral and buried inside in native structures.

Free energy of protein–ligand binding

According to the above results, the FMO partial charges have more influence on protein surface charge property than on protein stability. Therefore, the FMO partial charges might be more accurate in the simulations related to protein–ligand binding process. In this work, we test the FMO-RESP charges for the estimate of protein–ligand binding affinities for the two proteins. For dodecin, there are five ligands that are known to bind to the same site on its surface and that both complex crystal structures and binding affinities were experimentally characterized.[23] For lysozyme, we also select five ligands that are known to bind to the same site on its surface and that both complex crystal structures and binding affinities were experimentally characterized.[24,25]

To test the FMO-RESP partial charges, we calculated the free energies of protein–ligand binding using the MM-PBSA method with both the AMBER charges and the FMO-RESP charges. For ligands, we tested two sets of partial charges. One after the first stage of the fitting and the other after the second stage of the fitting (see Methodology for details).

The results are listed in Tables 1 and 2 and Figure 5. In the dodecin case, comparing to AMBER charges, the free energy values calculated using the FMO-RESP charges improves the prediction accuracy for experimental values. The correlation coefficients between computational and experimental values are 0.39 using the AMBER charges, 0.45 using the FMO-RESP charges (ligand charges are after the first stage), and 0.58 using the FMO-RESP charges (ligand charges are after the second stage RESP procedure). In the case of lysozyme, there is

Table 1. The free energy values (in kcal/mol) from experiments and computations with FMO-RESP charges and AMBER charges for dodecin.

Ligand	Experimental value	FMO-RESP charges	AMBER charges
FAD	−8.7	−13.0 (−10.3)	0.4
FMN	−6.6	−8.0 (−6.6)	−11.3
Riboflavin	−10.2	−12.2 (−15.2)	−19.9
Lumiflavin	−10.6	−13.9 (−13.5)	−14.9
Lumichrome	−10.9	−10.0 (−6.6)	−12.3

The data in brackets are values with ligand partial charges from first stage RESP fitting.

Table 2. The free energy values (in kcal/mol) from experiments and computations with FMO-RESP charges and AMBER charges for lysozyme.

Ligand	Experimental value	FMO-RESP charges	AMBER charges
NAG	−4.5	−22.6 (−19.4)	−6.3
NAG2	−7.2	−21.4 (−29.4)	−30.9
NAG3	−9.3	−41.1 (−35.9)	−37.6
NAG4	−9.6	−61.0 (−56.3)	−73.9
NAG-MUB	−4.1	−17.5 (−19.6)	−15.2

The data in brackets are values with ligand partial charges from first stage RESP fitting.

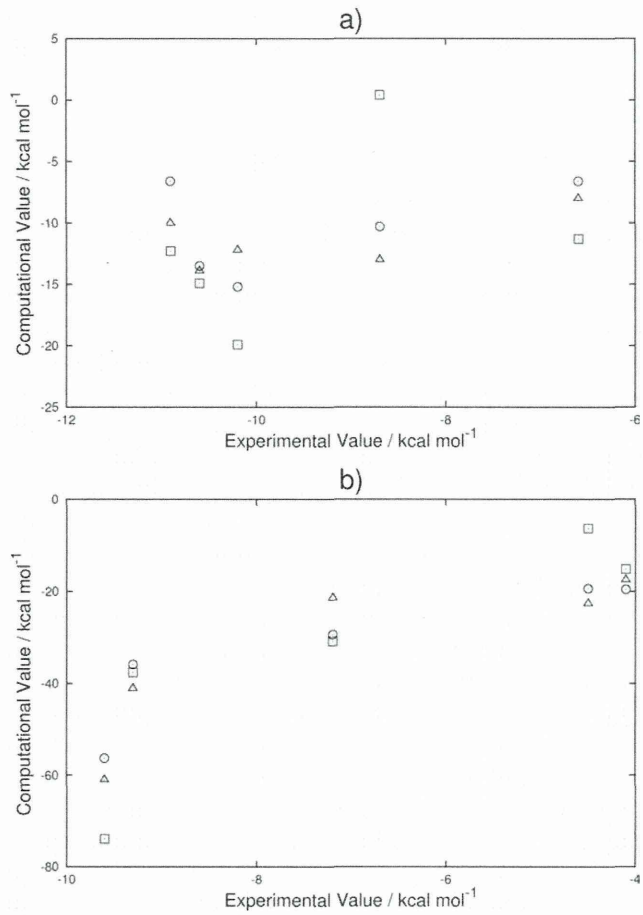

Figure 5. a) The correlations of binding free energies for the five dodecin-binding ligands between experimental values and computational values via different sets of partial charges. The correlation coefficients are 0.39 for AMBER charges (square), 0.45 for first stage FMO-RESP charges (circle), and 0.58 for second stage FMO-RESP charges (triangle). b) The correlations of binding free energies for the five lysozyme-binding ligands between experimental values and computational values via different sets of partial charges. The correlation coefficients are 0.87 for AMBER charges (square), 0.88 for first stage FMO-RESP charges (circle), and 0.85 for second stage FMO-RESP charges (triangle).

no obvious difference among the correlation coefficients between computational and experimental values, which are 0.87 using the AMBER charges, 0.88 using the FMO-RESP charges (ligand charges are after the first stage), and 0.85 using the FMO-RESP charges (ligand charges are after the second stage RESP procedure). Such results indicate the FMO-RESP charges could make better prediction for experimental protein–ligand binding free energies when the AMBER charges perform badly, and it would give equal level of prediction accuracy when the AMBER charges perform well.

Discussions

The current work is an initial trial to develop more accurate and efficient simulation methods to calculate ligand–protein binding affinities, and so there are apparently many rooms to improve it. Here, we discuss some issues.

First, in the current FMO-RESP procedure, we did not include solvent effect at all. We note that the AMBER 94 charges were determined by the electronic state calculations of molecules in vacuum. Thus, we followed the same procedure here. Technically, the inclusion of the implicit solvent model, such as the generalized Born model, is not difficult. However, the use of large dielectric constant for water tends to increase the amplitude of partial charges, which could cause serious issues when used in MD simulations. Thus, although the solvent effect is better to be taken into account in principle, it has to be done cautiously. To this direction, we need more thorough investigations.

Second, the charge distribution of ligand could alter during the binding process, especially for the charged ligand. In this work, we did not include the charge transfer between protein and ligand since the main purpose is to demonstrate the FMO charges is more accurate than AMBER charges in ligand–protein binding simulations. The discovery of more accurate ligand charges is not the main purpose. Besides, the FMO charges could give correct order of experimental binding affinities even for charged ligands FAD (−2e) and FMN (−1e), whereas AMBER charges could not. All the other ligands are neutral.

Third, the current work used a simple MM PBSA method to estimate binding free energies, which is obviously a very crude method. Here, we simply used it as a quick first trial. The accurate estimate of the binding free energy can be achieved by explicit calculations of the potential of mean force or other sampling simulations and by other methods. Moreover, accurate estimate of the binding affinity may require the use of explicit solvent water molecules. Both of them are much more time consuming and are postponed for our future study.

To be mentioned, the electrostatic potential in eq. 2 proposed by this paper is very useful in the analysis of large molecule interactions using FMO method. In general, the amplitude of the RESP charges depends on the strength of the restraint, which is modulated by the coefficient k. In this study, we simply followed an instruction given in Okiyama et al.[13] However, their purpose was not the ligand–protein binding affinity calculation and there is no guarantee that the same scheme works well. More careful investigation may be desired.

Conclusions

Applying the FMO-RESP method, we calculated protein-specific partial charges and then tested the charge set for protein–ligand binding free energy estimate for dodecin and lysozyme. We found some tendency of charge deviation from the standard AMBER charges: The partial charges are most markedly altered at isolated charged atoms. Even though the magnitude of charge deviation from the AMBER charge was relatively small, the use of FMO-RESP charge set improved the accuracy of the binding free energy for dodecin with five ligands.

Acknowledgments

This work was supported by Grant-in-Aid for Scientific Research, by Research and Development of the Next-Generation Integrated Simulation of Living Matter of the Ministry of Education Culture, Sports, Science and Technology (MEXT), and by the Global COE Program

'Formation of a Strategic Base for Biodiversity and Evolutionary Research: from Genome to Ecosystem' of the MEXT.

Keywords: fragment molecular orbital · molecular mechanics · *ab initio* molecular orbitals · *in silico* screening · restrained electrostatic potential

How to cite this article: L. Chang, T. Ishikawa, K. Kuwata, S. Takada, *J. Comput. Chem.* **2013,** *34,* 1251–1257. DOI: 10.1002/jcc.23250

[1] D. B. Kitchen, H. Decornez, J. R. Furr, J. Bajorath, *Nat. Rev. Drug Discov.* **2004**, *3,* 935.
[2] P. Ferrara, H. Gohlke, D. J. Price, G. Klebe, C. L. Brooks, III, J. Med. Chem. **2004**, *47,* 3032.
[3] S. J. Weiner, P. A. Kollman, D. A. Case, U. C. Singh, C. Ghio, G. Alagona, S. Profeta, Jr, P. Weiner, J. Am. *Chem. Soc.* **1984**, *106,* 765.
[4] S. J. Weiner, P. A. Kollman, D. T. Nguyen, D. A. Case, *J. Comput. Chem.* **1986**, *7,* 230.
[5] B. R. Brooks, R. E. Bruccoleri, B. D. Olafson, D. J. States, S. Swaminathan, M. Karplus, J. Comput. *Chem.* **1983**, *4,* 187.
[6] T. A. Halgren, W. Damm, Curr. Opin. Struct. Biol. **2001**, *11,* 236.
[7] Y. Tong, Y. Mei, Y. L. Li, C. G. Ji, J. Z. H. Zhang, J. Am. *Chem. Soc.* **2010**, *132,* 5137.
[8] Y. Mei, Y. L. Li, J. Zeng, J. Z. H. Zhang, J. Comput. *Chem.* **2012**, *33,* 1374.
[9] C. G. Ji, J. Z. H. Zhang, J. Comput. *Chem.* **2012**, *33,* 1416.
[10] Y. Xiang, L. Duan, J. Z. H. Zhang, J. Chem. *Phys.* **2011**, *134,* 205101.
[11] C. G. Ji, Y. Mei, J. Z. H. Zhang, Biophys. J. **2008**, *95,* 1080.
[12] Y. Okiyama, H. Watanabe, K. Fukuzawa, T. Nakano, Y. Mochizuki, T. Ishikawa, S. Tanaka, K. Ebina, *Chem. Phys. Lett.* **2007**, *449,* 329.
[13] Y. Okiyama, H. Watanabe, K. Fukuzawa, T. Nakano, Y. Mochizuki, T. Ishikawa, K. Ebina, S. Tanaka, Chem. Phys. Lett. **2009**, *467,* 417.
[14] K. Kitaura, E. Ikeo, T. Asada, T. Nakano, M. Uebayasi, *Chem. Phys. Lett.* **1999**, *313,* 701.
[15] M. S. Cordon, D. G. Fedorov, S. R. Pruitt, L. V. Slipchenko, *Chem. Rev.* **2012**, *112,* 632.
[16] M. W. Schmidt, K. K. Baldridge, J. A. Boatz, S. T. Elbert, M. S. Gordon, J. H. Jensen, S. Koseki, N. Matsunaga, K. A. Nguyen, S. J. Su, T. L. Windus, M. Dupuis, J. A. Montgomery, J. Comput. *Chem.* **1993**, *14,* 1347.
[17] D. G. Fedorov, K. Kitaura, J. Chem. *Phys.* **2004**, *120,* 6832.
[18] C. I. Bayly, P. Cieplak, W. D. Cornell, P. A. Kollman, J. Phys. *Chem.* **1993**, *97,* 10269.
[19] F.- Y.Dupradeau, A.Pigache, T.Zaffran, C.Savineau, R.Lelong, N.Grivel, D.Lelong, W.Rosanski, P.Cieplak, *Phys. Chem. Chem. Phys.* **2010**, *12,* 7821.
[20] D. A. Pearlman, D. A. Case, J. W. Caldwell, W. S. Ross, T. E. Cheatham, III, S. DeBolt, D. Ferguson, G. Seibel, P. Kollman, Comput. *Phys. Commun.* **1995**, *91,* 1.
[21] R. Luo, L. David, M. K. Gilson, J. Comput. *Chem.* **2002**, *23,* 1244.
[22] T. Ishikawa, K. Kuwata, J. Chem. Theory Comput. **2010**, *6,* 538.
[23] M. Grininger, K. Zeth, D. Oesterhelt, J. Mol. *Biol.* **2006**, *357,* 842.
[24] M. Schindler, Y. Assaf, N. Sharon, D. M. Chipman, *Biochemistry* **1977**, *16,* 423.
[25] K. Maenaka, M. Matsushima, H. Song, F. Sunada, K. Watanabe, I. Kumagai, J. Mol. *Biol.* **1995**, *247,* 281.

Received: 6 November 2012
Revised: 15 January 2013
Accepted: 22 January 2013, and final revision January 22, 2013
Published online on 19 February 2013